IEEE Access
Multidisciplinary : Rapid Review : Open Access Journal

Received September 18, 2020, accepted September 23, 2020, date of publication September 29, 2020, date of current version October 9, 2020.

Digital Object Identifier 10.1109/ACCESS.2020.3027686

Fixed-Time Adaptive Neural Control for Strict Feedback Nonlinear Systems via Event-Triggered Mechanism

XIN LIU, CHUANG GAO, MING CHEN, AND YONGHUI YANG
School of Electronic and Information Engineering, University of Science and Technology Liaoning, Anshan 114051, China

Corresponding author: Yonghui Yang (yangyh2636688@163.com)

This work was supported in part by the National Natural Science Foundation of China under Grant 61673199, Grant 21978123, Grant 71771112, and Grant 61403177.

ABSTRACT This article investigates an event-trigger-based fixed-time adaptive tracking control problem for strict feedback nonlinear systems with external disturbances. Relying on the values of the control input and tracking error, the relative fixed event-triggered control scheme is introduced to save communication resources on the basis of ensuring the control effect. Based on backstepping technology and neural network schemes, a fixed-time controller is devised to certify that the tracking error converges to a small neighborhood of the origin in the settling time. Meanwhile, all the signals of the closed-loop systems are bounded. The simulation results are presented to demonstrate the effectiveness of the proposed method.

INDEX TERMS Fixed-time stability, nonlinear systems, event-triggered mechanism, adaptive neural control, backstepping technology.

I. INTRODUCTION

Control theory has been widely developed and used in recent decades. Due to the continuous progress of computer technology, neural networks and fuzzy logic systems are recognized as efficacious strategies for unknown nonlinear systems [1]–[3]. Combined with backstepping technology, many developments have been made [4]–[9]. A controller devise problem was addressed for non-strict-feedback systems in [4]. [5] studied a robust fault estimation of discrete-time systems, and [6] investigated a class of control problems for multi-input multi-output (MIMO) unknown Euler-Lagrange systems with output constraints. In addition, [7] presented a fault-tolerant control strategy for leader-follower multiagent systems. Time delay problems in practical control systems were studied in [8] and [9]. These articles only prove the effectiveness of the control strategy and do not consider improvements in the transient performance and steady state performance of the system.

The required time for the controlled system from transient response to steady state response is also an important part of the controller design. To attain a shorter required time, [10] developed finite-time control techniques and applied them to a class of control systems. Combined with the Lyapunov theorem, finite-time control schemes have been obtained, such as [11]–[16]. References [11] and [12] researched the control problems for stochastic nonlinear systems. Reference [13] studied the finite-time control problem for multi-input multi-output (MIMO) feedback nonlinear systems, and [14] investigated multiagent systems. On the other hand, [15] devised homogeneous controllers for inverted pendulum systems. Combined with the adaptive fuzzy control scheme, the explosion of the complexity problem of the control system by the backstepping method was solved in [16]. Although this method makes the system achieve a steady state rapidly, it is necessary to know the initial state, and the practical applications will be limited. To expand the scope of the applications of this strategy, [17] developed the fixed-time scheme for the first time. Multiagent systems were discussed through the practical fixed-time control method in [18]–[20]. Based on the above schemes, [21] and [22] investigated an adaptive fixed-time controller with some fixed parameters and considered the constraint requirements of control systems. In these two articles, some parameters of the controller were fixed at the beginning of the design, and the parameters of the controller may not be set to the best

The associate editor coordinating the review of this manuscript and approving it for publication was Zhiguang Feng.

numerical values. Therefore, [23] proposed a new control method that can adjust all parameters of the controller freely. However, the partial controller needed to be approximated by the neural network, which may reduce the control accuracy. Moreover, [24] and [25] addressed the control problem for a class of nonlinear systems with dead-zone inputs.

The aforementioned achievements simply consider the performance problem of the control system without considering the resource utilization efficiency. The output of the controller in the traditional control strategy will be applied during the whole control process regardless of whether it is necessary. Communication will be congested if the network resources are limited. To save communication resources, researchers have proposed event-triggered mechanisms, such as [26]–[34]. Compared with the traditional event-triggered strategies, [26] and [27] addressed novel methods with inter-event times via additional internal dynamic variables. However, these controllers are investigated with the assumption of the input-to-state stability (ISS), and the application of the systems is limited. This means that fewer systems can be applied. To avoid this assumption, [28] proposed a novel method that concurrently designed adaptive and event-triggered strategies. By applying this strategy, [29] and [30] paid attention to stabilization issues for T-S fuzzy systems with discrete time and continuous time, respectively. An event-triggered observer was developed to investigate dynamic systems via the sliding mode surface method in [31]. Furthermore, a tracking control problem for nonlinear MIMO systems was studied in [32], and [33] addressed the distributed bipartite output consensus issue for multiagent systems. Reference [34] designed an adaptive event-triggered control strategy for nonlinear systems with a nonstrict feedback structure. Nevertheless, these strategies are based on a fixed threshold, which cannot take into account both the transient performance and the steady state performance of the system in the whole control process.

According to the aforementioned analysis, this article considers the tracking control problem of adaptive neural fixed-time control based on an event-trigger strategy for nonlinear systems through backstepping technology. The event-triggered strategy is presented to decrease the requirement for communication resources. The radial basis function neural networks (RBF NNs) are applied to approximate the uncertain terms in the nonlinear systems. Under the proposed method, the tracking error is guaranteed to converge to a small neighborhood of the origin within a settling-time interval. It is practically fixed-time stable for a class of closed-loop systems. The major features and contributions of this study are stated as follows:

(i) This article combines the fixed-time control scheme with the event-triggered strategy under backstepping technology. Compared with [23], the fixed-time control method for approximation by the RBF NNs is avoided, and the control accuracy is improved.

(ii) Based on the tracking error and a fixed value, an event-triggered strategy is proposed to reduce the requirement of communication resources in this article. The same threshold is applied to treat the transient process and steady state process of the system in Xing's event-triggered strategy [28], which limits the performance of the controller. Therefore, we propose a dynamic threshold based on the tracking error. Due to the large error in the initial stage of control, a small threshold is utilized to quickly reduce the error and to complete the tracking of the desired signal. After that, when the tracking error fluctuates in a small range, the threshold becomes larger and the unnecessary triggering is reduced. If the tracking error increases, the threshold decreases, and the control frequency is increased.

(iii) A single adaptive law is devised to reduce the computational burden of the device.

The remaining parts of this article are arranged as follows. A problem statement and several preliminaries are described in Section II. Section III proposes the event-trigger-based fixed-time adaptive controller. Through a numerical simulation example, Section IV verifies the effectiveness of the presented strategy. The conclusion is given in Section V.

II. PROBLEM STATEMENT AND PRELIMINARIES

A. PROBLEM FORMULATION

In this section, a class of strict-feedback nonlinear systems is expressed as follows:

$$\begin{cases} \dot{x}_i(t) = f_i(\bar{x}_i(t)) + g_i(\bar{x}_i(t))\,x_{i+1}(t) + d_i(t) \\ \dot{x}_n(t) = f_n(\bar{x}_n(t)) + g_n(\bar{x}_n(t))\,u(t) + d_n(t) \\ y(t) = x_1(t),\ i = 1,\cdots,n-1 \end{cases} \tag{1}$$

where $\bar{x}_i = [x_1,\cdots,x_i]^{\mathrm{T}} \in \Re^i$ are the state variables and $u(t) \in \Re$ and $y(t) \in \Re$ represent the input variable and the output variable, respectively. It can be assumed that $f_i(\cdot) : \Re^i \to \Re$ and $g_i(\cdot) : \Re^i \to \Re$ are the uncertain smooth functions with $g_i(0) = 0$ and $f_i(0) = 0$. The desired signal is devised by $y_d(t)$, which is a continuous differentiable function of any order. It is assumed that all the states of systems (1) must be completely measured as feedback state variables.

The objective of this article is to devise a fixed-time controller that satisfies several goals:

(a) All the signals remain semiglobally practically fixed-time bounded (SGPFB).

(b) The tracking error between $y(t) \in \Re$ and $y_d(t)$ converges to a small neighborhood of the origin in a settling time without needing the initial conditions.

(c) An event-triggered scheme is established to decrease the requirement for communication resources.

B. DEFINITION, LEMMAS AND ASSUMPTION

Definition 1 [17]: The following nonlinear system is considered:

$$\dot{x} = f(x,t) \tag{2}$$

with $x(0) = x_0$. $x \in \Re^n$ is the state vector, and $f(\cdot) : \Re_+ \times \Re^n \to \Re^n$ is the continuous function. For any initial condition $x(0) \in \Omega$. It is assumed that the solution of system $\|x(t, x_0)\| \leq \iota$ converges to compact Ω within finite time T, which satisfies $T \leq T_{\max}$. The origin of system (2) is considered to be semiglobally practically fixed-time stability (SPFTS).

Lemma 1 [35]: Assuming the following design constants: $p, q > 0$, $0 < \mu < 1$ and $\beta > 1$, it is obtained that

$$\dot{V}(x) \leq -pV^{\mu}(x) - qV^{\beta}(x) \tag{3}$$

where $\dot{V}(x)$ expresses a Lyapunov function. The fixed time for system (2), which is stable at the origin, satisfies

$$T \leq T_{\max} := \frac{1}{(1-\mu)p\varphi} + \frac{1}{(\beta-1)q\varphi}. \tag{4}$$

Lemma 2 [23]: Suppose that several design constants satisfy $p, q > 0$, $0 < \mu < 1$, $\beta > 1$ and $0 < \Delta < +\infty$; it follows that

$$\dot{V}(x) \leq -pV^{\mu}(x) - qV^{\beta}(x) + \Delta \tag{5}$$

which ensures the practical fixed-time stability of system (2). If there exists a design parameter $0 < \varphi < 1$, then the settling time can be given by

$$T \leq T_{\max} := \frac{1}{(1-\mu)p\varphi} + \frac{1}{(\beta-1)q\varphi}. \tag{6}$$

The residual set of the solution in system (2) is expressed as

$$x \in \left\{ V(x) \leq \min\left\{ \left(\frac{\Delta}{(1-\varphi)q}\right)^{\frac{1}{\beta}}, \left(\frac{\Delta}{(1-\varphi)p}\right)^{\frac{1}{\mu}} \right\} \right\}. \tag{7}$$

Lemma 3 [36]: For any real variables ψ and ξ, the following holds:

$$|\psi|^{b_1}|\xi|^{b_2} \leq \frac{b_1}{b_1+b_2} b_3 |\psi|^{b_1+b_2} + \frac{b_2}{b_1+b_2} b_3^{-\frac{b_1}{b_2}} |\xi|^{b_1+b_2} \tag{8}$$

where b_1, b_2 and b_3 are positive constants.

Lemma 4 [37]: On the assumption that $\Theta_i \in \Re$, the following holds:

$$(|\Theta_1| + \cdots + |\Theta_n|)^{\tau} \leq |\Theta_1|^{\tau} + \cdots + |\Theta_n|^{\tau} \tag{9}$$

with $\tau \in [0, 1]$, $i = 1, \cdots, n$.

Lemma 5 [38]: If any parameter p satisfies $0 < p < 1$, it follows that

$$\left(\sum_{j=1}^{n} |\varsigma_j|^2\right)^{\frac{1+p}{2}} \leq \sum_{j=1}^{n} |\varsigma_j|^{1+p}. \tag{10}$$

Lemma 6 [21]: If there exists a parameter $\varsigma_i \geq 0$, we have

$$\left(\sum_{j=1}^{n} \varsigma_j\right)^2 \leq n \sum_{j=1}^{n} \varsigma_j^2 \tag{11}$$

with $i = 1, \cdots, n$.

Lemma 7 [39]: If there exists a continuous function $f(Q) : \Re^n \to \Re$, which is defined on a compact set Φ, it can be approximated by the RBF NNs $W^{\mathrm{T}}S(Q)$ such that

$$\bar{f}(Q) = W^{\mathrm{T}}S(Q) + \delta(Q). \tag{12}$$

The ideal constant weight is described by $W = [w_1, \cdots w_l] \in \Re^l$, and l is the number of nodes from the RBF NNs. $S(Q) = [s_1(Q), \cdots, s_l(Q)]^{\mathrm{T}}$ represents the basis function vector by $s_i(Q) = \exp\left(-\|Q - o_i\|^2/r^2\right)$. The Gaussian functions are centered at o_i, and $r > 0$ expresses the Gaussian width. Approximation error $\delta(Q)$ satisfies $|\delta(Q)| \leq \varepsilon$, where $\varepsilon > 0$ is a constant.

Lemma 8 [40]: For any constant $\vartheta \in \Re$ and $\sigma > 0$, we have

$$0 < |\vartheta| - \vartheta \tanh\left(\frac{\vartheta}{\sigma}\right) \leq 0.2785\sigma. \tag{13}$$

Lemma 9 (Young's Inequality): If real numbers $\epsilon_1 > 1$ and $\epsilon_2 > 1$ satisfy $1/\epsilon_1 + 1/\epsilon_2 = 1$, for any vectors γ and υ, the inequality holds:

$$\gamma^{\mathrm{T}}\upsilon \leq \frac{h^{\epsilon_1}}{\epsilon_1}\|\gamma\|^{\epsilon_1} + \frac{1}{\epsilon_2 h^{\epsilon_2}}\|\upsilon\|^{\epsilon_2} \tag{14}$$

with $h > 0$.

Assumption 1: If the sign of function $g_i(\bar{x}_i)$ never changes, it can be obtained by

$$0 < b_m \leq g_i(\bar{x}_i) \leq b_M < +\infty \tag{15}$$

where b_m and b_M are constants and $i = 1, \cdots, n$.

By simplifying notation, time variable t and state variable $\bar{x}_i$ are omitted in the related functions.

III. MAIN RESULTS

A. FIXED-TIME CONTROLLER DESIGN

The design process of the adaptive fixed-time controller through the event-triggered strategy for system (1) is established with backstepping technology, and the relative results can be obtained in this section.

Based on backstepping technology, the coordinate transformation can be obtained by

$$z_1 = x_1 - y_d \tag{16}$$

and

$$z_i = x_i - \alpha_{i-1} \tag{17}$$

where α_{i-1} represents the virtual control law. The virtual control law is defined by

$$\alpha_i = -p_i\left(\frac{1}{2}\right)^{\mu} z_i^{2\mu-1} - q_i\left(\frac{1}{2}\right)^{\beta} z_i^{2\beta-1} - \frac{1}{4a_i^2} z_i \hat{\theta} S_i^{\mathrm{T}}(Q_i) S_i(Q_i) \tag{18}$$

where $0.5 < \mu < 1$ and $\beta > 1$ are constants and p_i, q_i are positive regulated parameters. Furthermore, the adaptive controller is chosen by

$$v(t) = \alpha_n - \bar{\omega} \tanh\left(\frac{z_n \bar{\omega}}{\sigma}\right) \tag{19}$$

where $\bar{\omega}$ and σ are positive constants. The adaptive law is devised by

$$\dot{\hat{\theta}} = \sum_{i=1}^{n} \frac{b_m}{4a_i^2} z_i^2 S_i^{\mathrm{T}}(Q_i) S_i(Q_i) - \rho\hat{\theta} \tag{20}$$

where $b_m, \rho, a_i > 0$ are the regulated parameters, and adaptive parameter $\hat{\theta}$ represents the estimation of constant $\theta = \max\left\{\|W_i\|^2/b_m, i = 1, \cdots, n\right\}$. According to Lemma 7, the functions $S_i(Q_i)$ are utilized to approximate the unknown nonlinear functions with $Q_1 = \left[x_1, y_d^{(0)}, y_d^{(1)}\right]^{\mathrm{T}}$ and $Q_i = \left[\bar{x}_i^{\mathrm{T}}, \theta, y_d^{(0)}, \cdots, y_d^{(i)}\right]^{\mathrm{T}}$.

Step 1

Based on (16), the time derivative of z_1 is given by

$$\begin{aligned} \dot{z}_1 &= \dot{x}_1 - \dot{y}_d \\ &= f_1 + g_1 x_2 + d_1 - \dot{y}_d. \end{aligned} \tag{21}$$

The Lyapunov function is described as

$$V_1 = \frac{1}{2} z_1^2 + \frac{b_m}{2\zeta}\tilde{\theta}^2 \tag{22}$$

where ζ is a positive constant, and the evaluated error of θ can be devised by $\tilde{\theta} = \theta - \hat{\theta}$. Differentiating V_1 in (22) with respect to time produces

$$\begin{aligned} \dot{V}_1 &= z_1\dot{z}_1 - \frac{b_m}{\zeta}\tilde{\theta}\dot{\hat{\theta}} \\ &= z_1(f_1 + g_1 x_2 + d_1 - \dot{y}_d) - \frac{b_m}{\zeta}\tilde{\theta}\dot{\hat{\theta}} \\ &= z_1 f_1 + z_1 g_1 z_2 + z_1 g_1 \alpha_1 + z_1 d_1 - z_1\dot{y}_d - \frac{b_m}{\zeta}\tilde{\theta}\dot{\hat{\theta}} \\ &= z_1 \bar{f}_1 - \frac{b_m}{\zeta}\tilde{\theta}\dot{\hat{\theta}} + z_1 g_1 z_2 + z_1 g_1 \alpha_1 - \frac{z_1^2}{2} + z_1 d_1 \end{aligned} \tag{23}$$

where $\bar{f}_1 = f_1 - \dot{y}_d + z_1/2$ replaces the unknown package term. According to Lemma 7, $\bar{f}_1$ is approximated by

$$\bar{f}_1 = W_1^{\mathrm{T}} S_1(Q_1) + \delta_1(Q_1) \tag{24}$$

such that

$$\begin{aligned} z_1\bar{f}_1 &= z_1\left(W_1^{\mathrm{T}} S_1(Q_1) + \delta_1(Q_1)\right) \\ &\le |z_1|\,\|W_1\|\,\|S_1(Q_1)\| + |z_1|\,\varepsilon_1 \\ &\le \frac{1}{4a_1^2} z_1^2 \|W_1\|^2 \|S_1(Q_1)\|^2 + a_1^2 + \frac{1}{4} z_1^2 + \varepsilon_1^2 \\ &= \frac{b_m}{4a_1^2} z_1^2 \theta \|S_1(Q_1)\|^2 + a_1^2 + \frac{1}{4} z_1^2 + \varepsilon_1^2 \end{aligned} \tag{25}$$

where $\varepsilon_1 \ge |\delta_1|$ is a positive constant. It is easily seen from Lemma 9 that

$$z_1 d_1 \le \frac{1}{4} z_1^2 + \bar{d}_1^2 \tag{26}$$

where $\bar{d}_1$ is a positive constant and satisfies $\bar{d}_1 \ge |d_1|$. Substituting (25) and (26) into (23) gives

$$\begin{aligned} \dot{V}_1 \le{}& \frac{b_m}{4a_1^2} z_1^2 \theta \|S_1(Q_1)\|^2 + a_1^2 + \varepsilon_1^2 + \bar{d}_1^2 \\ & - \frac{b_m}{\zeta}\tilde{\theta}\dot{\hat{\theta}} + z_1 g_1 z_2 + z_1 g_1 \alpha_1. \end{aligned} \tag{27}$$

According to (15) and (18), the term $z_1 g_1 \alpha_1$ in (27) can be written as

$$\begin{aligned} z_1 g_1 \alpha_1 &= -g_1 p_1 \left(\frac{1}{2} z_1^2\right)^{\mu} - g_1 q_1 \left(\frac{1}{2} z_1^2\right)^{\beta} \\ &\quad - \frac{g_1}{4a_1^2} z_1^2 \hat{\theta} S_1^{\mathrm{T}}(Q_1) S_1(Q_1) \\ &\le -b_m p_1 \left(\frac{1}{2} z_1^2\right)^{\mu} - b_m q_1 \left(\frac{1}{2} z_1^2\right)^{\beta} \\ &\quad - \frac{b_m}{4a_1^2} z_1^2 \hat{\theta} S_1^{\mathrm{T}}(Q_1) S_1(Q_1). \end{aligned} \tag{28}$$

Substituting (28) into (27), the following is obtained:

$$\begin{aligned} \dot{V}_1 \le{}& \frac{b_m}{4a_1^2} z_1^2 \theta \|S_1(Q_1)\|^2 + a_1^2 + \varepsilon_1^2 + \bar{d}_1^2 - \frac{b_m}{\zeta}\tilde{\theta}\dot{\hat{\theta}} \\ & + z_1 g_1 z_2 - b_m p_1 \left(\frac{1}{2} z_1^2\right)^{\mu} - b_m q_1 \left(\frac{1}{2} z_1^2\right)^{\beta} \\ & - \frac{b_m}{4a_1^2} z_1^2 \hat{\theta} S_1^{\mathrm{T}}(Q_1) S_1(Q_1) \\ ={}& -b_m p_1 \left(\frac{1}{2} z_1^2\right)^{\mu} - b_m q_1 \left(\frac{1}{2} z_1^2\right)^{\beta} + z_1 g_1 z_2 + a_1^2 \\ & + \frac{b_m}{\zeta}\tilde{\theta}\left(\frac{\zeta}{4a_1^2} z_1^2 \|S_1(Q_1)\|^2 - \dot{\hat{\theta}}\right) + \varepsilon_1^2 + \bar{d}_1^2. \end{aligned} \tag{29}$$

Step *i* $(i = 2, \cdots, n-1)$

According to (17), the time derivative of z_i can be obtained by

$$\begin{aligned} \dot{z}_i &= \dot{x}_i - \dot{\alpha}_{i-1} \\ &= f_i + g_i x_{i+1} + d_i - \dot{\alpha}_{i-1} \end{aligned} \tag{30}$$

where $\dot{\alpha}_{i-1} = \sum_{j=1}^{i-1} \frac{\partial \alpha_{i-1}}{\partial x_j} f_j + \sum_{j=0}^{i-1} \frac{\partial \alpha_{i-1}}{\partial y_d^{(j)}} y_d^{(j+1)} + \frac{\partial \alpha_{i-1}}{\partial \hat{\theta}}\dot{\hat{\theta}}$. For the ith subsystem in (1), the following candidate form of the Lyapunov function can be described as

$$V_i = \frac{1}{2} z_i^2 + V_{i-1}. \tag{31}$$

According to (30), the time derivative of $\dot{V}_i$ is given by

$$\begin{aligned} \dot{V}_i &= z_i\dot{z}_i + \dot{V}_{i-1} \\ &\le z_i f_i + z_i g_i z_{i+1} + z_i g_i \alpha_i + z_i d_i - z_i\dot{\alpha}_{i-1} + z_{i-1} g_{i-1} z_i \\ &\quad - b_m \sum_{j=1}^{i-1} p_j \left(\frac{z_j^2}{2}\right)^{\mu} - b_m \sum_{j=1}^{i-1} q_j \left(\frac{z_j^2}{2}\right)^{\beta} + \sum_{j=1}^{i-1} a_j^2 \end{aligned}$$

$$
\begin{aligned}
&+\frac{b_m\tilde{\theta}}{\zeta}\left(\sum_{j=1}^{i-1}\frac{\zeta z_j^2}{4a_j^2}\|S_j(Q_j)\|^2-\dot{\hat{\theta}}\right)+\sum_{j=1}^{i-1}\varepsilon_j^2+\sum_{j=1}^{i-1}\bar{d}_j^2\\
\le{}& z_i\bar{f}_i-\frac{1}{2}z_i^2+z_ig_iz_{i+1}+z_ig_i\alpha_i+z_id_i+\sum_{j=1}^{i-1}\bar{d}_j^2\\
&-b_m\sum_{j=1}^{i-1}p_j\left(\frac{z_j^2}{2}\right)^{\mu}-b_m\sum_{j=1}^{i-1}q_j\left(\frac{z_j^2}{2}\right)^{\beta}+\sum_{j=1}^{i-1}a_j^2\\
&+\frac{b_m\tilde{\theta}}{\zeta}\left(\sum_{j=1}^{i-1}\frac{\zeta z_j^2}{4a_j^2}\|S_j(Q_j)\|^2-\dot{\hat{\theta}}\right)+\sum_{j=1}^{i-1}\varepsilon_j^2 \qquad (32)
\end{aligned}
$$

where $\bar{f}_i=f_i+z_i/2-\dot{\alpha}_{i-1}+z_{i-1}g_{i-1}$. Based on Lemma 7, the term $z_i\bar{f}_i$ in (32) is written as

$$
\begin{aligned}
z_i\bar{f}_i&=z_i\left(W_i^{\mathrm{T}}S_i(Q_i)+\delta_i(Q_i)\right)\\
&\le|z_i|\,\|W_i\|\,\|S_i(Q_i)\|+|z_i|\,\varepsilon_i\\
&\le\frac{1}{4a_i^2}z_i^2\|W_i\|^2\|S_i(Q_i)\|^2+a_i^2+\frac{1}{4}z_i^2+\varepsilon_i^2\\
&=\frac{b_m}{4a_i^2}z_i^2\theta\|S_i(Q_i)\|^2+a_i^2+\frac{1}{4}z_i^2+\varepsilon_i^2 \qquad (33)
\end{aligned}
$$

where $\varepsilon_i\ge|\delta_i|$ is a positive constant. Applying Lemma 9, the following holds:

$$
z_id_i\le\frac{1}{4}z_i^2+\bar{d}_i^2 \qquad (34)
$$

where $\bar{d}_i$ is a positive parameter with $\bar{d}_i\ge|d_i|$. Substituting (33) and (34) into (32) gives

$$
\begin{aligned}
\dot{V}_i\le{}&\frac{b_m}{4a_i^2}z_i^2\theta\|S_i(Q_i)\|^2+z_ig_iz_{i+1}+z_ig_i\alpha_i+\sum_{j=1}^{i}\varepsilon_j^2\\
&-b_m\sum_{j=1}^{i-1}p_j\left(\frac{z_j^2}{2}\right)^{\mu}-b_m\sum_{j=1}^{i-1}q_j\left(\frac{z_j^2}{2}\right)^{\beta}+\sum_{j=1}^{i}\bar{d}_j^2\\
&+\frac{b_m}{\zeta}\tilde{\theta}\left(\sum_{j=1}^{i-1}\frac{\zeta z_j^2}{4a_j^2}\|S_j(Q_j)\|^2-\dot{\hat{\theta}}\right)+\sum_{j=1}^{i}a_j^2. \qquad (35)
\end{aligned}
$$

According to (15) and (18), the term $z_ig_i\alpha_i$ from (35) can be described as

$$
\begin{aligned}
z_ig_i\alpha_i={}&-g_ip_i\left(\frac{z_i^2}{2}\right)^{\mu}-g_iq_i\left(\frac{z_i^2}{2}\right)^{\beta}\\
&-\frac{1}{4a_i^2}g_iz_i^2\hat{\theta}S_i^{\mathrm{T}}(Q_i)S_i(Q_i)\\
\le{}&-b_mp_i\left(\frac{z_i^2}{2}\right)^{\mu}-b_mq_i\left(\frac{z_i^2}{2}\right)^{\beta}\\
&-\frac{b_m}{4a_i^2}z_i^2\hat{\theta}S_i^{\mathrm{T}}(Q_i)S_i(Q_i). \qquad (36)
\end{aligned}
$$

Combining (35) and (36), we have

$$
\begin{aligned}
\dot{V}_i\le{}&-b_m\sum_{j=1}^{i}p_j\left(\frac{z_j^2}{2}\right)^{\mu}-b_m\sum_{j=1}^{i}q_j\left(\frac{z_j^2}{2}\right)^{\beta}+\sum_{j=1}^{i}a_j^2\\
&+z_ig_iz_{i+1}+\frac{b_m}{\zeta}\tilde{\theta}\left(\sum_{j=1}^{i}\frac{\zeta z_j^2}{4a_j^2}\|S_j(Q_j)\|^2-\dot{\hat{\theta}}\right)\\
&+\sum_{j=1}^{i}\varepsilon_j^2+\sum_{j=1}^{i}\bar{d}_j^2. \qquad (37)
\end{aligned}
$$

Step *n*

Similar to **Step 1** and **Step *i***, the coordinate transformation is given by

$$
z_n=x_n-\alpha_{n-1} \qquad (38)
$$

and the time derivative of z_n is obtained by

$$
\begin{aligned}
\dot{z}_n&=\dot{x}_n-\dot{\alpha}_{n-1}\\
&=f_n+g_nu+d_n-\dot{\alpha}_{n-1} \qquad (39)
\end{aligned}
$$

where $\dot{\alpha}_{n-1}=\sum_{j=1}^{n-1}\frac{\partial\alpha_{n-1}}{\partial x_j}f_j+\sum_{j=0}^{n-1}\frac{\partial\alpha_{i-1}}{\partial y_d^{(j)}}y_d^{(j+1)}+\frac{\partial\alpha_{n-1}}{\partial\hat{\theta}}\dot{\hat{\theta}}$. Consider the following Lyapunov function candidate for the nth subsystem:

$$
V_n=\frac{1}{2}z_n^2+V_{n-1}. \qquad (40)
$$

The time derivative of V_n is expressed as

$$
\begin{aligned}
\dot{V}_n={}&z_n\dot{z}_n+\dot{V}_{n-1}\\
\le{}&z_nf_n+z_ng_nu+z_nd_n-z_n\dot{\alpha}_{n-1}\\
&-b_m\sum_{j=1}^{n-1}p_j\left(\frac{z_j^2}{2}\right)^{\mu}-b_m\sum_{j=1}^{n-1}q_j\left(\frac{z_j^2}{2}\right)^{\beta}\\
&+z_{n-1}g_{n-1}z_n+\frac{b_m\tilde{\theta}}{\zeta}\left(\sum_{j=1}^{n-1}\frac{\zeta z_j^2}{4a_j^2}\|S_j(Q_j)\|^2-\dot{\hat{\theta}}\right)\\
&+\sum_{j=1}^{n-1}a_j^2+\sum_{j=1}^{n-1}\varepsilon_j^2+\sum_{j=1}^{n-1}\bar{d}_j^2\\
={}&z_n\bar{f}_n-\frac{1}{2}z_n^2+z_ng_nu+z_nd_n+\sum_{j=1}^{n-1}a_j^2+\sum_{j=1}^{n-1}\varepsilon_j^2\\
&+\sum_{j=1}^{n-1}\bar{d}_j^2-b_m\sum_{j=1}^{n-1}p_j\left(\frac{z_j^2}{2}\right)^{\mu}-b_m\sum_{j=1}^{n-1}q_j\left(\frac{z_j^2}{2}\right)^{\beta}\\
&+\frac{b_m\tilde{\theta}}{\zeta}\left(\sum_{j=1}^{n-1}\frac{\zeta z_j^2}{4a_j^2}\|S_j(Q_j)\|^2-\dot{\hat{\theta}}\right) \qquad (41)
\end{aligned}
$$

where $\bar{f}_n=f_n+z_n/2-\dot{\alpha}_{n-1}+z_{n-1}g_{n-1}$. According to Lemma 7, term $z_n\bar{f}_n$ in (41) is written as

$$
\begin{aligned}
z_n\bar{f}_n&=z_n\left(W_n^{\mathrm{T}}S_n(Q_n)+\delta_n(Q_n)\right)\\
&\le|z_n|\,\|W_n\|\,\|S_n(Q_n)\|+|z_n|\,\varepsilon_n\\
&\le\frac{1}{4a_n^2}z_n^2\|W_n\|^2\|S_n(Q_n)\|^2+a_n^2+\frac{1}{4}z_n^2+\varepsilon_n^2\\
&=\frac{b_m}{4a_n^2}z_n^2\theta\|S_n(Q_n)\|^2+a_n^2+\frac{1}{4}z_n^2+\varepsilon_n^2 \qquad (42)
\end{aligned}
$$

where $\varepsilon_n \geq |\delta_n|$ is a positive constant. From Lemma 9, the term can be described as

$$z_n d_n \leq \frac{1}{4} z_n^2 + \bar{d}_n^2 \tag{43}$$

where $\bar{d}_n \geq |d_n|$ is a positive parameter. Combining (41), (42) and (43) results in

$$\begin{aligned}\dot{V}_n \leq & \frac{b_m}{4a_n^2} z_n^2 \theta \|S_n(Q_n)\|^2 + z_n g_n u \\ & - b_m \sum_{j=1}^{n-1} p_j \left(\frac{z_j^2}{2}\right)^{\mu} - b_m \sum_{j=1}^{n-1} q_j \left(\frac{z_j^2}{2}\right)^{\beta} \\ & + \frac{b_m}{\zeta} \tilde{\theta} \left(\sum_{j=1}^{n-1} \frac{\zeta z_j^2}{4a_j^2} \|S_j(Q_j)\|^2 - \dot{\hat{\theta}} \right) \\ & + \sum_{j=1}^{n} a_j^2 + \sum_{j=1}^{n} \bar{d}_j^2 + \sum_{j=1}^{n} \varepsilon_j^2. \end{aligned} \tag{44}$$

The tracking control problem from system (1) has been preliminarily settled. Nonetheless, real-time control will occupy unnecessary communication resources. Hence, a proposed event-triggered strategy is introduced as follows.

B. TRACKING ERROR BASED FIXED THRESHOLD STRATEGY

To attain the objective of the event-triggered control, [28] designed a fixed threshold strategy. From this work, we consider the influence of tracking error on the triggering events, and the proposed strategy can be expressed as follows:

$$\begin{cases} v(t) = \alpha_n - \bar{\omega} \tanh\left(\frac{z_n \bar{\omega}}{\sigma}\right) \\ u(t) = v(t_k), \quad \forall t \in [t_k, t_{k+1}), \ t_1 = 0 \\ t_{k+1} = \inf\{t \in \Re \,|\, |\kappa(t)| \geq \omega^*\} \end{cases} \tag{45}$$

where $\bar{\omega}$ is a positive constant, and the term $\bar{\omega}\tanh(z_n\bar{\omega}/\sigma)$ in controller (45) is used to avoid the ISS assumption with measurement error. $\kappa(t) = v(t) - u(t)$ represents the measuring error. We select a positive constant $\bar{t}$, which satisfies $\bar{t} \leq \{t_{k+1} - t_k\}$ with $\forall k \in z^+$. From the derivative of $\kappa(t)$, it is obtained that

$$\frac{d}{dt}|\kappa| = \frac{d}{dt}(\kappa * \kappa)^{\frac{1}{2}} = \operatorname{sign}(\kappa)\dot{\kappa} \leq |\dot{v}|. \tag{46}$$

For (45), the time derivative of v can be given by

$$\dot{v} = \dot{\alpha}_n - \frac{\bar{\omega}\dot{z}_n}{\cosh^2\left(\frac{z_n\bar{\omega}}{\sigma}\right)}. \tag{47}$$

The above shows that the functions $f_i(\bar{x}_i)$, $g_i(\bar{x}_i)$, and $d_i(t)$ are at least $(n+1-i)$th order smooth functions, and desired signal $y_d(t)$ has $(n+1)$th order continuous derivatives; hence, $\dot{v}$ must be continuous. Furthermore, a positive constant ϕ must exist with $\phi \geq |\dot{v}|$. From (46), we obtain $\kappa(t_k) = 0$ and $\lim_{t \to t_{k+1}} (\kappa(t)) = \omega^*$. Hence, the lower bound of inter-execution intervals $\bar{t}$ satisfies $\bar{t} \geq \omega^*/\phi$. Therefore, the Zeno behavior is completely avoided. Event-triggered threshold ω^* is obtained by

$$\omega^* = \frac{\omega_1}{\omega_2 + \omega_4 |z_1(t)|} + \omega_3 \tag{48}$$

where ω_1, ω_2, ω_3 and ω_4 are positively designed parameters. The continuous control input signal is expressed as $v(t) = u(t) + \eta(t)\omega^*$, where $\eta(t)$ is a continuous time-varying parameter satisfying $|\eta(t)| \leq 1$, $\eta(t_k) = 0$, and $\eta(t_{k+1}) = \pm 1$. Substituting (18), (45) and (48), the term $z_n g_n \alpha_n$ in (44) is described as

$$\begin{aligned} z_n g_n u &= z_n g_n \left(v(t) - \eta(t)\omega^*\right) \\ &= z_n g_n \alpha_n - z_n g_n \bar{\omega} \tanh\left(\frac{z_n\bar{\omega}}{\sigma}\right) - z_n g_n \eta(t)\omega^* \\ &\leq z_n g_n \alpha_n - z_n g_n \bar{\omega} \tanh\left(\frac{z_n\bar{\omega}}{\sigma}\right) + g_n |z_n \bar{\omega}|. \end{aligned} \tag{49}$$

To keep the function continuous and smooth, we utilize the properties of inequality from Lemma 8 instead of the term with absolute values in (49) as follows:

$$\begin{aligned} z_n g_n u &\leq z_n g_n \alpha_n + 0.2785\sigma \\ &\leq -b_m p_n \left(\frac{1}{2}z_n^2\right)^{\mu} - b_m q_n \left(\frac{1}{2}z_n^2\right)^{\beta} \\ &\quad - \frac{b_m}{4a_n^2} z_n^2 \hat{\theta} S_n^{\mathrm{T}}(Q_n) S_n(Q_n) + 0.2785\sigma. \end{aligned} \tag{50}$$

Substituting (20) and (50) into (44) produces

$$\begin{aligned} \dot{V}_n \leq & \frac{b_m z_n^2}{4a_n^2} \theta \|S_n(Q_n)\|^2 - b_m p_n \left(\frac{z_n^2}{2}\right)^{\mu} - b_m q_n \left(\frac{z_n^2}{2}\right)^{\beta} \\ & - \frac{b_m}{4a_n^2} z_n^2 \hat{\theta} S_n^{\mathrm{T}}(Q_n) S_n(Q_n) + 0.2785\sigma + \frac{b_m\rho}{\zeta}\tilde{\theta}\hat{\theta} \\ & + \frac{b_m}{\zeta}\tilde{\theta} \left(\sum_{j=1}^{n-1} \frac{\zeta z_j^2}{4a_j^2} \|S_j(Q_j)\|^2 - \sum_{j=1}^{n} \frac{\zeta z_j^2}{4a_j^2} \|S_j(Q_j)\|^2 \right) \\ & + \sum_{j=1}^{n} a_j^2 + \sum_{j=1}^{n} \bar{d}_j^2 + \sum_{j=1}^{n} \varepsilon_j^2 \\ = & -b_m \sum_{j=1}^{n} p_j \left(\frac{z_j^2}{2}\right)^{\mu} - b_m \sum_{j=1}^{n} q_j \left(\frac{z_j^2}{2}\right)^{\beta} + \frac{b_m\rho}{\zeta}\tilde{\theta}\hat{\theta} \\ & + 0.2785\sigma + \sum_{j=1}^{n} a_j^2 + \sum_{j=1}^{n} \varepsilon_j^2 + \sum_{j=1}^{n} \bar{d}_j^2. \end{aligned} \tag{51}$$

C. STABILITY ANALYSIS

According to Lyapunov theory, the conclusion of convergence analysis can be obtained in this subsection.

From Lemma 9, the term $\rho b_m \tilde{\theta}\hat{\theta}/\zeta$ in (51) can be obtained

$$\begin{aligned} \frac{b_m\rho}{\zeta}\tilde{\theta}\hat{\theta} &\leq -\frac{b_m\rho}{2\zeta}\tilde{\theta}^2 + \frac{b_m\rho}{2\zeta}\theta^2 \\ &= -\frac{1}{2}\left(\frac{b_m\rho}{2\zeta}\tilde{\theta}^2\right) - \frac{1}{2}\left(\frac{b_m\rho}{2\zeta}\tilde{\theta}^2\right) + \frac{b_m\rho}{2\zeta}\theta^2. \end{aligned} \tag{52}$$

It can be assumed that adaptive law θ is bounded by an unknown constant Δ_θ satisfying $|\theta| \le \Delta_\theta$. If $\Delta_\theta < \sqrt{2\zeta/\rho b_m}$, we have

$$-\frac{1}{2}\left(\frac{b_m\rho}{2\zeta}\tilde{\theta}^2\right) \le -\frac{1}{2}\left(\frac{b_m\rho}{2\zeta}\tilde{\theta}^2\right)^\beta. \tag{53}$$

Otherwise, while $\Delta_\theta \ge \sqrt{2\zeta/\rho b_m}$, it is easily proven that

$$\begin{aligned}-\frac{1}{2}\left(\frac{b_m\rho}{2\zeta}\tilde{\theta}^2\right) &\le -\frac{1}{2}\left(\frac{b_m\rho}{2\zeta}\tilde{\theta}^2\right)+\frac{1}{2}\left(\frac{b_m\rho}{2\zeta}\Delta_\theta^2\right)^\beta \\ &\quad -\frac{1}{2}\left(\frac{b_m\rho}{2\zeta}\tilde{\theta}^2\right)^\beta \\ &= -\frac{1}{2}\left(\frac{b_m\rho}{2\zeta}\tilde{\theta}^2\right)^\beta + \Delta_1\end{aligned} \tag{54}$$

where $\Delta_1 = \left(b_m\rho\Delta_\theta^2/2\zeta\right)^\beta/2 - \left(b_m\rho\tilde{\theta}^2/2\zeta\right)/2 \ge 0$. As stated in Lemma 3, while $\psi = 1$, $\xi = 0.5b_m\tilde{\theta}^2/\zeta$, $b_1 = 1-\mu$, $b_2 = \mu$, and $b_3 = \exp\left((\mu/(1-\mu))\ln\mu\right)$, it can be shown that

$$\left(\frac{b_m}{2\zeta}\tilde{\theta}^2\right)^\mu \le (1-\mu)\,\mu^{\frac{\mu}{1-\mu}} + \frac{b_m}{2\zeta}\tilde{\theta}^2. \tag{55}$$

In addition, it is easily seen from (55) that

$$-\frac{\rho}{2}\frac{b_m}{2\zeta}\tilde{\theta}^2 \le -\frac{\rho}{2}\left(\frac{b_m}{2\zeta}\tilde{\theta}^2\right)^\mu + \frac{\rho}{2}(1-\mu)\,\mu^{\frac{\mu}{1-\mu}}. \tag{56}$$

Substituting (53), (54) and (56) into (52) produces

$$\begin{aligned}\frac{b_m\rho}{\zeta}\tilde{\theta}\hat{\theta} \le -\frac{\rho}{2}\left(\frac{b_m}{2\zeta}\tilde{\theta}^2\right)^\mu - \frac{\rho}{2n}\left(\frac{b_m}{2\zeta}\tilde{\theta}^2\right)^\beta \\ + \frac{\rho b_m}{2\zeta}\theta + \frac{\rho}{2}(1-\mu)\,\mu^{\frac{\mu}{1-\mu}}.\end{aligned} \tag{57}$$

Applying Lemma 4, Lemma 5 and Lemma 6, the following is verified:

$$-\sum_{j=1}^{n} p_j\left(\frac{z_j^2}{2}\right)^\mu \le -\chi_1\sum_{j=1}^{n}\left(\frac{z_j^2}{2}\right)^\mu \le -\chi_1\left(\sum_{j=1}^{n}\frac{z_j^2}{2}\right)^\mu \tag{58}$$

and

$$-\sum_{j=1}^{n} q_j\left(\frac{z_j^2}{2}\right)^\beta \le -\chi_2\sum_{j=1}^{n}\left(\frac{z_j^2}{2}\right)^\beta \le -\frac{\chi_2}{n}\left(\sum_{j=1}^{n}\frac{z_j^2}{2}\right)^\beta \tag{59}$$

where $\chi_1 = \min\left\{p_j \,|j = 1,\cdots,n\right\}$, and $\chi_2 = \min\left\{q_j \,|j = 1,\cdots,n\right\}$. Due to the parameters satisfying $b_m, \rho, \mu, a_j, \varepsilon_j, \bar{d}_j, \sigma > 0$, combining (57), (58) and (59) results in the following inequality:

$$\begin{aligned}\dot{V}_n \le{}& -b_m\chi_1\left(\sum_{j=1}^{n}\frac{z_j^2}{2}\right)^\mu - \frac{\rho}{2}\left(\frac{b_m}{2\zeta}\tilde{\theta}^2\right)^\mu \\ & -\frac{b_m\chi_2}{n}\left(\sum_{j=1}^{n}\frac{z_j^2}{2}\right)^\beta - \frac{\rho}{2n}\left(\frac{b_m}{2\zeta}\tilde{\theta}^2\right)^\beta \\ & + \frac{\rho b_m}{2\zeta}\theta + \frac{\rho}{2}(1-\mu)\,\mu^{\frac{\mu}{1-\mu}} + \sum_{j=1}^{n} a_j^2 \\ & + \sum_{j=1}^{n}\varepsilon_j^2 + \sum_{j=1}^{n}\bar{d}_j^2 + 0.2785\sigma + \Delta_1 \\ ={}& -c_1V_n^\mu - c_2V_n^\beta + \Delta\end{aligned} \tag{60}$$

where $c_1 = \min\{b_m\chi_1, \rho/2\}$, $c_2 = \min\{b_m\chi_2/n, \rho/2n\}$, and $\Delta = 0.5\rho(1-\mu)\,\mu^{\mu/(1-\mu)} + \sum_{j=1}^{n} a_j^2 + \sum_{j=1}^{n}\bar{d}_j^2 + \sum_{j=1}^{n}\varepsilon_j^2 + 0.2785\sigma + \Delta_1$. By utilizing Lemma 2, all of the signals in the closed-loop system (1) are guaranteed to be SPFTCs. The signals can converge to the compact set

$$x \in \left\{V(x) \le \min\left\{\left(\frac{\Delta}{(1-\varphi)q}\right)^{\frac{1}{\beta}}, \left(\frac{\Delta}{(1-\varphi)p}\right)^{\frac{1}{\mu}}\right\}\right\}. \tag{61}$$

The tracking error can be accommodated into a small region satisfying

$$|y - y_d| \le 2\left(\frac{\Delta}{(1-\varphi)q}\right)^{\frac{1}{2\beta}}, \tag{62}$$

and the fixed time is selected with

$$T \le T_{\max} := \frac{1}{(1-\mu)p\varphi} + \frac{1}{(\beta-1)q\varphi}. \tag{63}$$

At present, based on backstepping technology, the adaptive fixed-time controller has been designed completely via the proposed event-triggered strategy. Fig. 1 shows the diagram of the design procedure of the controller. The proposed event-triggered strategy and fixed-time method are devised based on state feedback. To achieve the purpose of design, the information is received and sent through the micro controller unit.

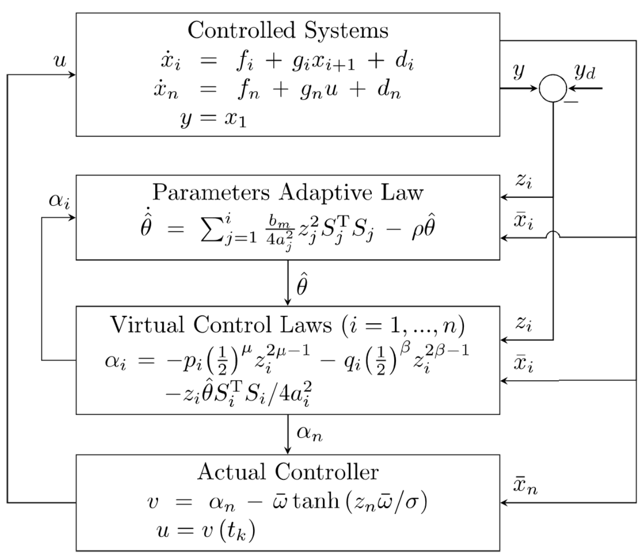

FIGURE 1. The block diagram of the design procedure for the proposed controller.

IV. SIMULATION RESULTS

The system model [39] is expressed as

$$\begin{cases} \dot{x}_1(t) = f_1(x_1(t)) + g_1(x_1(t))\, x_2(t) + d_1(t) \\ \dot{x}_2(t) = f_2(\bar{x}_2(t)) + g_2(\bar{x}_2(t))\, u(t) + d_2(t) \\ y(t) = x_1(t) \end{cases} \tag{64}$$

where $f_1(x_1(t)) = 0.1x_1^2(t)$, $f_2(\bar{x}_2(t)) = 0.1x_1(t)\, x_2(t) - 0.2x_1(t)$, $g_1(x_1(t)) = 1$ and $g_2(\bar{x}_2(t)) = 1 + x_1^2(t)$. The external disturbances are $d_1(t) = 0.1\sin x_1(t)\cos x_1(t)$ and $d_2(t) = \cos x_1(t)\sin x_2(t)$. The initial values of each state variable are given by $x_1(0) = 1$ and $x_2(0) = -1$. The control purpose is to devise the event-triggered fixed-time adaptive control strategy to ensure the output signal $y(t)$ to track the given signal $y_d(t) = (\sin(t/2) + \sin(t))/2$. The controller is defined by

$$v(t) = \alpha_2 - \bar{\omega}\tanh\left(\frac{z_2\bar{\omega}}{\sigma}\right). \tag{65}$$

The triggering event can be described as

$$u(t) = v(t_k), \quad \forall t \in [t_k, t_{k+1}) \tag{66}$$

where $t_{k+1} = \inf\{t \in \Re \mid |\kappa(t)| \geq \omega^*\}$ and $t_1 = 0$. The virtual control laws can be obtained with

$$\alpha_1 = -p_1\left(\frac{1}{2}\right)^{\mu} z_1^{2\mu-1} - q_1\left(\frac{1}{2}\right)^{\beta} z_1^{2\beta-1} - \frac{z_1\hat{\theta}}{4a_1^2} S_1^{\mathrm{T}}(Q_1)\, S_1(Q_1) \tag{67}$$

and

$$\alpha_2 = -p_2\left(\frac{1}{2}\right)^{\mu} z_2^{2\mu-1} - q_2\left(\frac{1}{2}\right)^{\beta} z_2^{2\beta-1} - \frac{z_2\hat{\theta}}{4a_2^2} S_2^{\mathrm{T}}(Q_2)\, S_2(Q_2) \tag{68}$$

where RBF NNs $W_1^{\mathrm{T}} S_1(Q_1)$ and $W_2^{\mathrm{T}} S_2(Q_2)$ are utilized to approximate the uncertain nonlinear functions from system (64), where $S_1 = [x_1, y_d, \dot{y}_d]^{\mathrm{T}}$ and $S_2 = [x_1, x_2, \theta, y_d, \dot{y}_d, \ddot{y}_d]^{\mathrm{T}}$. The Gaussian functions are centered at $[0, 1, -1, 3, -3, 5, -5, 7, -7]^{\mathrm{T}}$. In addition, the Gaussian width is $r = 2$. The adaptive law is described by

$$\dot{\hat{\theta}} = \sum_{j=1}^{n} \frac{b_m}{4a_j^2} z_j^2 S_j^{\mathrm{T}}(Q_j)\, S_j(Q_j) - \rho\hat{\theta}. \tag{69}$$

The simulation parameters of the virtual control laws, actual control law and adaptive laws are selected within the interval (0, 50). To achieve good performance, the related design parameters can be selected as $\mu = 3/4$, $\beta = 3/2$, $p_1 = 16$, $p_2 = 22$, $q_1 = q_2 = 2$, $a_1 = a_2 = 2$, $b_m = 20$ and $\rho = 20$. The parameters of the two strategies are as follows: a. Proposed strategy: $\bar{\omega} = 12$, $\omega_1 = 0.7$, $\omega_2 = 0.14$, $\omega_3 = 3.5$ and $\omega_4 = 50$; b. Fixed threshold strategy: $\bar{\omega} = 12$ and $\omega_3 = 8.5$.

The simulation results are shown in Figs. 2-8. The trajectories of desired signal y_d and the actual state variables

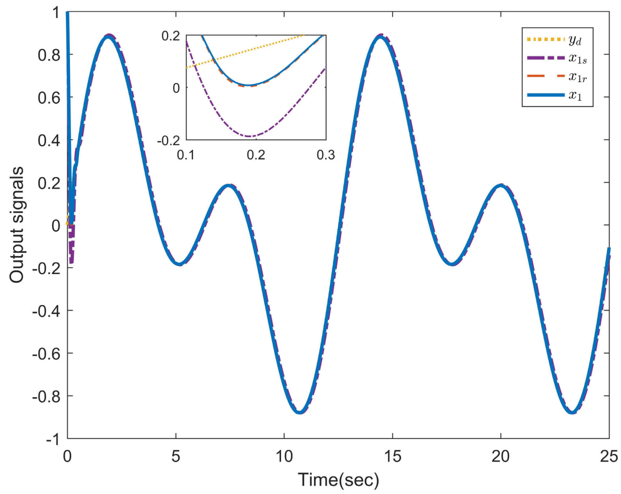

FIGURE 2. **The trajectories of the tracking signal y_d and the states x_{1s}, x_{1r}, x_1 under different controllers.**

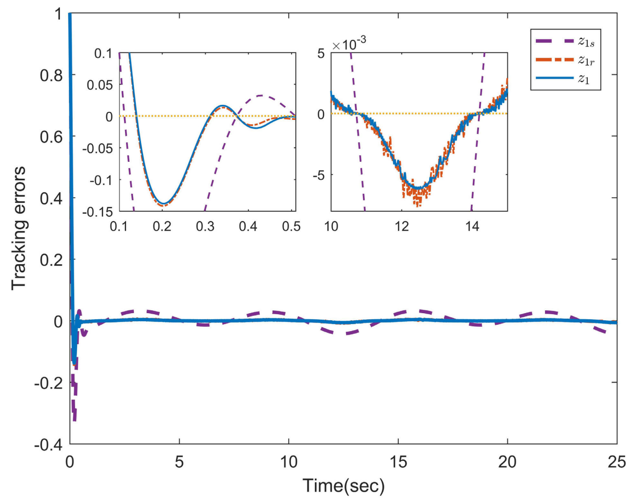

FIGURE 3. **The trajectory of the tracking error of x_{1s}, x_{1r} and x_1.**

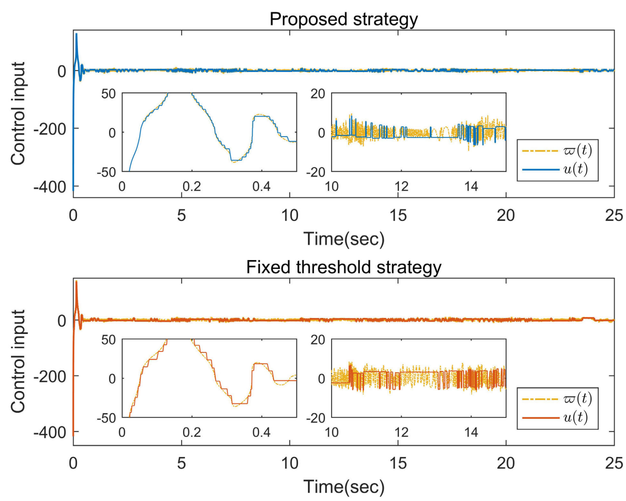

FIGURE 4. **Control signals of proposed strategy and fixed threshold strategy.**

are displayed in Fig. 2. x_{1s} is the tracking effect of general adaptive neural control. x_{1r} and x_1 show the tracking

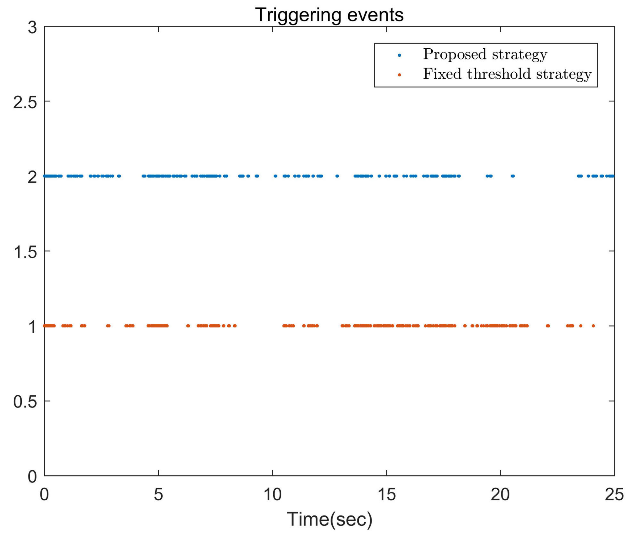

FIGURE 5. Triggered events of proposed strategy and fixed threshold strategy.

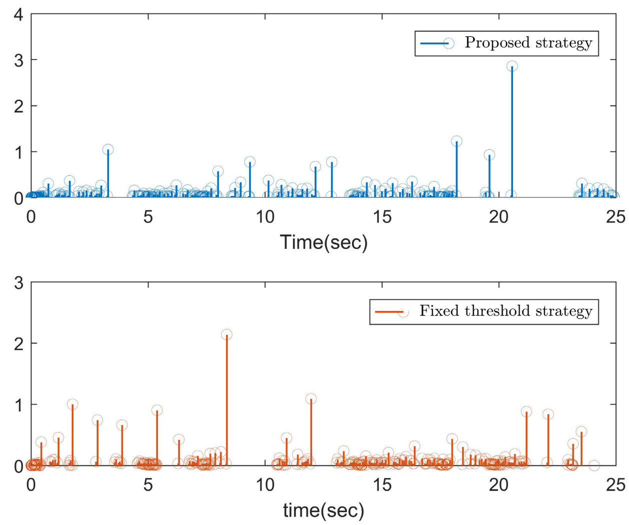

FIGURE 6. Time intervals of triggered events in proposed strategy and fixed threshold strategy.

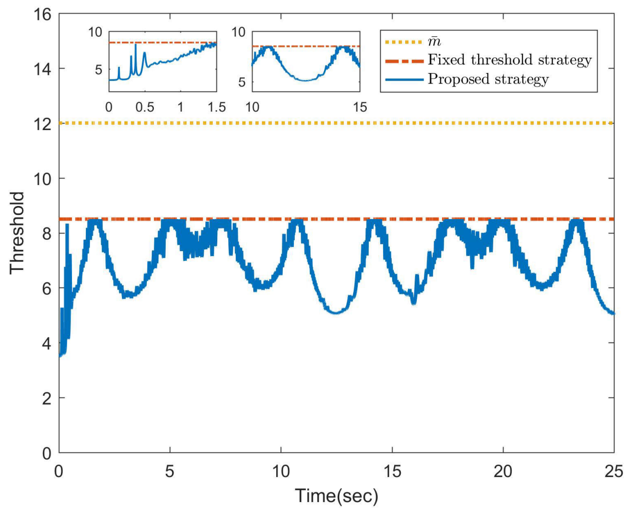

FIGURE 7. Comparison of threshold values between proposed strategy and fixed threshold strategy.

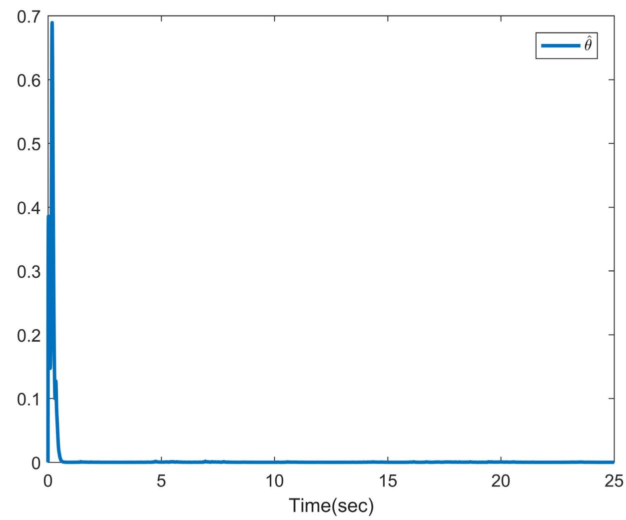

FIGURE 8. The trajectory of adaptive law θ from the proposed strategy.

effect based on the fixed-time adaptive neural controller via Xing's event-triggered strategy and the proposed strategy [28]. Under the same control parameters, the fixed-time method takes less time to reach the steady state performance. The tracking errors of various strategies are shown in Fig. 3. The error of the proposed strategy, z_1 has a smaller maximum overshoot, and the tracking error is smaller than z_{1s} and z_{1r}. Fig. 4 shows the trajectories of the control signals between the proposed threshold control scheme and the fixed threshold control scheme. In the initial stage of the control, the threshold value of the proposed strategy is smaller and triggers more times than that of Xing's strategy, which causes the tracking error to decrease rapidly. The numbers of triggering events in 0.5 seconds are 98 and 72, respectively. Furthermore, the proposed strategy can adjust the trigger threshold appropriately with the tracking error and maintains the error in a small range near the origin. During the whole control process, the total numbers of triggering events are 379 and 360. Figs. 5 and 6 present the triggering times and the triggering values of these schemes. The threshold values of the two schemes are shown in Fig. 7. Compared with the fixed threshold, the proposed threshold is smaller at the beginning of control and increases with a decrease in the tracking error. After 1.5 seconds, the system reaches a steady state, and the threshold fluctuates with z_1. This ensures that while the tracking error increases, the number of trigger times grows. When the tracking error becomes 0, the threshold of the proposed strategy increases to the maximum and is the same as the fixed threshold. Finally, the trajectory of the adaptive law is presented in Fig. 8. It starts at zero and gradually decreases. The results verify that the closed-loop system is a SPFTC, and the tracking error converges in the settling time.

V. CONCLUSION

By applying backstepping technology, this article developed a fixed-time event-triggered adaptive neural control strategy for strict feedback nonlinear systems with external disturbances. According to the transformation state error-based fixed threshold method, the event-triggered controller is devised to ensure the effective utilization of communication resources. Under the proposed control strategy, the closed-loop system satisfies the SPFTS requirement. The tracking error converges in the settling time. Meanwhile, all the signals of the closed-loop system are bounded. Finally, the proposed scheme is feasible and effective in the simulation results.

REFERENCES

[1] A. Wu and Z. Zeng, "Dynamic behaviors of memristor-based recurrent neural networks with time-varying delays," *Neural Netw.*, vol. 36, pp. 1–10, Dec. 2012.

[2] A. Wu and Z. Zeng, "Exponential stabilization of memristive neural networks with time delays," *IEEE Trans. Neural Netw. Learn. Syst.*, vol. 23, no. 12, pp. 1919–1929, Dec. 2012.

[3] A. Wu and Z. Zeng, "Global Mittag–Leffler stabilization of fractional-order memristive neural networks," *IEEE Trans. Neural Netw. Learn. Syst.*, vol. 28, no. 1, pp. 206–217, Jan. 2017.

[4] H. Wang, S. Liu, and X. Yang, "Adaptive neural control for non-strict-feedback nonlinear systems with input delay," *Inf. Sci.*, vol. 514, pp. 605–616, Apr. 2020.

[5] X. Xie, H. Yuan, D. Yue, and J. Cao, "Robust fault estimation of discrete-time nonlinear system based on an enhanced maximum-priority-based switching law," *J. Franklin Inst.*, vol. 357, no. 8, pp. 5073–5090, May 2020.

[6] J.-X. Zhang and G.-H. Yang, "Fault-tolerant output-constrained control of unknown Euler–Lagrange systems with prescribed tracking accuracy," *Automatica*, vol. 111, Jan. 2020, Art. no. 108606.

[7] Z. Wang, Y. Wu, L. Liu, and H. Zhang, "Adaptive fault-tolerant consensus protocols for multiagent systems with directed graphs," *IEEE Trans. Cybern.*, vol. 50, no. 1, pp. 25–35, Jan. 2020.

[8] Z. Feng and W. X. Zheng, "Improved stability condition for Takagi–Sugeno fuzzy systems with time-varying delay," *IEEE Trans. Cybern.*, vol. 47, no. 3, pp. 661–670, Mar. 2017.

[9] Z. Feng, W. X. Zheng, and L. Wu, "Reachable set estimation of T–S fuzzy systems with time-varying delay," *IEEE Trans. Fuzzy Syst.*, vol. 25, no. 4, pp. 878–891, Aug. 2017.

[10] S. P. Bhat and D. S. Bernstein, "Continuous finite-time stabilization of the translational and rotational double integrators," *IEEE Trans. Autom. Control*, vol. 43, no. 5, pp. 678–682, May 1998.

[11] F. Wang, B. Chen, Y. Sun, Y. Gao, and C. Lin, "Finite-time fuzzy control of stochastic nonlinear systems," *IEEE Trans. Cybern.*, vol. 50, no. 6, pp. 2617–2626, Jun. 2020.

[12] Y. Sun, B. Mao, S. Zhou, and H. Liu, "Finite-time adaptive control for non-strict feedback stochastic nonlinear systems," *IEEE Access*, vol. 7, pp. 179758–179764, 2019.

[13] Y. Li, K. Li, and S. Tong, "Finite-time adaptive fuzzy output feedback dynamic surface control for MIMO nonstrict feedback systems," *IEEE Trans. Fuzzy Syst.*, vol. 27, no. 1, pp. 96–110, Jan. 2019.

[14] J. Duan, H. Zhang, Y. Cai, and K. Zhang, "Finite-time time-varying output formation-tracking of heterogeneous linear multi-agent systems," *J. Franklin Inst.*, vol. 357, no. 2, pp. 926–941, Jan. 2020.

[15] T. Yang and Y. Li, "Finite-time control for a class of inverted pendulum systems," *IEEE Access*, vol. 7, pp. 129637–129643, 2019.

[16] H. Wang, S. Kang, and Z. Feng, "Finite-time adaptive fuzzy command filtered backstepping control for a class of nonlinear systems," *Int. J. Fuzzy Syst.*, vol. 21, no. 8, pp. 2575–2587, Oct. 2019.

[17] A. Polyakov, "Nonlinear feedback design for fixed-time stabilization of linear control systems," *IEEE Trans. Autom. Control*, vol. 57, no. 8, pp. 2106–2110, Aug. 2012.

[18] Z. Zuo, Q.-L. Han, B. Ning, X. Ge, and X.-M. Zhang, "An overview of recent advances in fixed-time cooperative control of multiagent systems," *IEEE Trans. Ind. Informat.*, vol. 14, no. 6, pp. 2322–2334, Jun. 2018.

[19] B. Ning, Q.-L. Han, and Q. Zuo, "Distributed optimization for multiagent systems: An edge-based fixed-time consensus approach," *IEEE Trans. Cybern.*, vol. 49, no. 1, pp. 122–132, Jan. 2019.

[20] B. Ning, Q. Han, and Q. Zuo, "Practical fixed-time consensus for integrator-type multi-agent systems: A time base generator approach," *Automatica*, vol. 105, no. 1, pp. 122–132, Jul. 2019.

[21] X. Jin, "Adaptive fixed-time control for MIMO nonlinear systems with asymmetric output constraints using universal barrier functions," *IEEE Trans. Autom. Control*, vol. 64, no. 7, pp. 3046–3053, Jul. 2019.

[22] Q. Zhou, P. Du, H. Li, R. Lu, and J. Yang, "Adaptive fixed-time control of error-constrained pure-feedback interconnected nonlinear systems," *IEEE Trans. Syst., Man, Cybern. Syst.*, early access, Jan. 10, 2020, doi: 10.1109/TSMC.2019.2961371.

[23] D. Ba, Y.-X. Li, and S. Tong, "Fixed-time adaptive neural tracking control for a class of uncertain nonstrict nonlinear systems," *Neurocomputing*, vol. 363, pp. 273–280, Oct. 2019.

[24] C. Hua, Y. Li, and X. Guan, "Finite/fixed-time stabilization for nonlinear interconnected systems with dead-zone input," *IEEE Trans. Autom. Control*, vol. 62, no. 5, pp. 2554–2560, May 2017.

[25] Z. Zhang, X. Liu, Y. Liu, C. Lin, and B. Chen, "Fixed-time almost disturbance decoupling of nonlinear time-varying systems with multiple disturbances and dead-zone input," *Inf. Sci.*, vol. 450, pp. 267–283, Jun. 2018.

[26] A. Girard, "Dynamic triggering mechanisms for event-triggered control," *IEEE Trans. Autom. Control*, vol. 60, no. 7, pp. 1992–1997, Jul. 2015.

[27] R. Postoyan, P. Tabuada, D. Nesic, and A. Anta, "A framework for the event-triggered stabilization of nonlinear systems," *IEEE Trans. Autom. Control*, vol. 60, no. 4, pp. 982–996, Apr. 2015.

[28] L. Xing, C. Wen, Z. Liu, H. Su, and J. Cai, "Event-triggered adaptive control for a class of uncertain nonlinear systems," *IEEE Trans. Autom. Control*, vol. 62, no. 4, pp. 2071–2076, Apr. 2017.

[29] X. Xie, Q. Zhou, D. Yue, and H. Li, "Relaxed control design of discrete-time Takagi–Sugeno fuzzy systems: An event-triggered real-time scheduling approach," *IEEE Trans. Syst., Man, Cybern. Syst.*, vol. 48, no. 12, pp. 2251–2262, Dec. 2018.

[30] N. Rong and Z. Wang, "Fixed-time stabilization for IT2 T–S fuzzy interconnected systems via event-triggered mechanism: An exponential gain method," *IEEE Trans. Fuzzy Syst.*, vol. 28, no. 2, pp. 246–258, Feb. 2020.

[31] X. Liu, X. Su, P. Shi, C. Shen, and Y. Peng, "Event-triggered sliding mode control of nonlinear dynamic systems," *Automatica*, vol. 112, Feb. 2020, Art. no. 108738.

[32] Y.-X. Li, G.-H. Yang, and S. Tong, "Event-triggered adaptive fuzzy tracking control of nonlinear MIMO systems," *Int. J. Syst. Sci.*, vol. 49, no. 12, pp. 2618–2629, Aug. 2018.

[33] Y. Cai, H. Zhang, Y. Liu, and Q. He, "Distributed bipartite finite-time event-triggered output consensus for heterogeneous linear multi-agent systems under directed signed communication topology," *Appl. Math. Comput.*, vol. 378, Aug. 2020, Art. no. 125162.

[34] W. Wang, Y. Li, and S. Tong, "Neural-network-based adaptive event-triggered consensus control of nonstrict-feedback nonlinear systems," *IEEE Trans. Neural Netw. Learn. Syst.*, early access, May 18, 2020, doi: 10.1109/TNNLS.2020.2991015.

[35] Z. Zuo, B. Tian, M. Defoort, and Z. Ding, "Fixed-time consensus tracking for multiagent systems with high-order integrator dynamics," *IEEE Trans. Autom. Control*, vol. 63, no. 2, pp. 563–570, Feb. 2018.

[36] C. Qian and W. Lin, "Non-lipschitz continuous stabilizers for nonlinear systems with uncontrollable unstable linearization," *Syst. Control Lett.*, vol. 42, no. 3, pp. 185–200, Mar. 2001.

[37] Z. Zhu, Y. Xia, and M. Fu, "Attitude stabilization of rigid spacecraft with finite-time convergence," *Int. J. Robust Nonlinear Control*, vol. 21, no. 6, pp. 686–702, Apr. 2011.

[38] S. Yu, X. Yu, B. Shirinzadeh, and Z. Man, "Continuous finite-time control for robotic manipulators with terminal sliding mode," *Automatica*, vol. 41, no. 11, pp. 1957–1964, Nov. 2005.

[39] L.-X. Wang and J. M. Mendel, "Fuzzy basis functions, universal approximation, and orthogonal least-squares learning," *IEEE Trans. Neural Netw.*, vol. 3, no. 5, pp. 807–814, Sep. 1992.

[40] M. M. Polycarpou and P. A. Ioannou, "A robust adaptive nonlinear control design," in *Proc. Amer. Control Conf.*, Jun. 1993, pp. 1365–1369.

XIN LIU received the B.Sc. degree in electrical engineering and automation from the University of Science and Technology Liaoning, Anshan, China, in 2015, where he is currently pursuing the M.S. degree in control engineering. His research interests include fuzzy control, adaptive control, and control of nonlinear time-delay systems.

CHUANG GAO received the B.S. degree in electronic and communication engineering from the University of Warwick, Coventry, U.K., in 2005, the M.S. degree in digital signal processing from King's College London, U.K., in 2007, and the Ph.D. degree in iron and steel metallurgy from the University of Science and Technology Liaoning, Anshan, China, in 2020. He has authored over 20 research articles indexed by SCI and EI. His research interests include nonlinear system control, machine learning, and intelligent control.

MING CHEN received the B.Sc. degree in automation from the Anshan Iron and Steel Institute, Anshan, China, in 2000, the M.Sc. degree in control theory and control engineering from the University of Science and Technology Liaoning, Anshan, China, in 2004, and the Ph.D. degree in control theory and control engineering from the University of Science and Technology Beijing, Beijing, China, in 2009. She is currently a Professor with the School of Electronic and Information Engineering, University of Science and Technology Liaoning. Her research interests include nonlinear control systems, robust control, and fault tolerant control.

YONGHUI YANG received the B.Sc. degree in computer science from Northeastern University, Shenyang, China, in 1995, and the M.Sc. degree in electronic and information engineering and the Ph.D. degree in chemical engineering from the University of Science and Technology Liaoning, Anshan, China, in 2010 and 2018, respectively. He is currently a Professor with the School of Electronic and Information Engineering, University of Science and Technology Liaoning. His research interests include nonlinear control, intelligent process control, robot communication and control, and machine learning.